THE ASTROPHYSICAL JOURNAL, 356:416–429, 1990 June 20

A TEST OF THE ASSOCIATION OF INFRARED ACTIVITY WITH BARS[1]

STEPHEN M. POMPEA AND G. H. RIEKE
Steward Observatory, University of Arizona
Received 1989 June 6; accepted 1989 December 20

ABSTRACT

The hypothesis that high far-infrared luminosities in noninteracting galaxies are dependent on material fed into their nuclei or into circumnuclear rings along bars can be tested by near-infrared imaging. Except in extreme starbursts, the near-infrared emission arises from the stars that dominate the mass of the stellar populations; moreover, the effects of interstellar extinction are greatly reduced at these wavelengths compared with the visible. We have selected a sample of 22 galaxies from the Revised Shapley-Ames Catalog that have far-infrared luminosities $>10^{10}\ L_{\odot}$ and hot colors between 60 and 100 μm ($S_{60}/S_{100} > 0.5$), indicative of possible nuclear starbursts, but are not interacting or classified as Seyfert galaxies. Fifteen galaxies of the sample of 16 that are not clearly barred from optical data and are isolated were imaged at 1.6 and 2.2 μm. In an evaluation of the infrared images, at least eight of these galaxies do not appear to have bars. Strong bars therefore do not appear to be an absolute requirement for high infrared luminosity.

Subject headings: galaxies: structures — infrared: sources

I. INTRODUCTION

Bars are common structures in galaxies; 35% of the galaxies of type S0 to type Sc in the Revised Shapley-Ames Catalog (Sandage and Tammann 1981, hereafter RSA) are classified as barred. A variety of numerical modeling experiments (e.g., Sellwood 1981) have shown that bars readily form from instabilities in an initially axisymmetric disk. Thus bars are easily created and are stable over many galaxy rotation periods. Bars can drive noncircular motions of gas; gas orbiting through the outer part of a bar can be concentrated in a ring at the end of a bar. Gas in the inner part of a bar sinks to the galactic center as it loses energy and angular momentum in shocks (Roberts, Huntley, and van Albada 1979). Norman (1987) shows how bars can drive an outward angular momentum flow and an inward mass flow toward the nucleus.

Hawarden *et al.* (1986) and Puxley *et al.* (1987) suggest that nearly all noninteracting galaxies (excluding those with Seyfert type spectra) with a 25 μm excess are barred. They argue that the 25 μm excesses are indicative of high infrared luminosities due to recent star formation, which is fueled by gas funneled into a circumnuclear ring or the nucleus by the bar. Their conclusions are extended to an optically selected sample of starburst galaxies by Arsenault (1989). Devereux (1987*b*) find a correlation between enhanced 10 μm central ($\sim$1 kpc diameter) luminosity and the presence of bars in early-type infrared luminous galaxies. However, in late-type spirals, Devereux finds no strong dependence of the infrared luminosity on barred morphology. Barred galaxies have been observed in radio continuum emission at the VLA by Hummel, van der Hulst, and Dickey (1984), who showed that the enhancement in star formation is confined to a region near the center (less than 20″) or to a nuclear ring, if it was resolved. The presence of an optical bar in spirals is correlated with increased infrared luminosity. Hawarden *et al.* (1986) showed that the total infrared luminosity of barred galaxies in a sample of RC2 galaxies (which excluded low-ionization nuclei emission regions [LINERS]) was about twice that ($4.3 \times 10^{10}\ L_{\odot}$) of the unbarred galaxies in the sample ($L = 1.7 \times 10^{10}\ L_{\odot}$).

However, it is unclear whether bars or interaction are an absolute requirement to allow adequate quantities of gas to settle into the nuclear region for a moderate to high-luminosity starburst. Optical searches for weak bars or oval distortions are hampered by large amounts of extinction, even in galaxies with low inclination. Hawarden *et al.* (1986) suggested that the 25 μm excess galaxies in their sample that were not classified as barred probably have obscured bars. Observations in the Gunn *i* band to search for bars (Zaritsky and Lo 1986) represent a considerable improvement over visible measurements. Observations in the near-infrared near 2 μm further reduce the obscuration due to dust and delineate more clearly the underlying, old stellar population that dominates the gravitational potential. Thus a range of galaxies with different inclinations and central obscurations can be studied. This paper presents 1.6 and 2.2 μm images of a sample of galaxies from the RSA that have characteristics of nuclear starbursts and analyzes them for the presence of bars.

II. SAMPLE SELECTION AND OBSERVATIONS

We selected a sample of galaxies for near-IR imaging in a series of steps. First, galaxies were selected from the RSA which had the ratio of band 3 to band 4 *IRAS* fluxes greater than 0.5 and far-infrared luminosity greater than $10^{10}\ L_{\odot}$ (calculated as in Rieke and Lebofsky 1986). Seyfert 1 and 2 galaxies were eliminated from the list using a catalog of known Seyfert galaxies (Véron-Cetty and Véron 1987). The remaining galaxies were examined on Palomar Sky Survey plates to eliminate those with companions within 1.5 galaxy diameters or with obvious signs of interaction, such as tidal tails or highly distorted disks. Galaxies with possible merger or interaction signs, such as bright knots in the disk, were not eliminated. In a final step only galaxies north of declination $-30°$ (to be observable from $+32°$ latitude) were included. These criteria lead to a complete sample of 22 galaxies, of which six were clearly barred in optical photographs. The 16 optically unbarred or marginally barred galaxies constituted our final observing list as given in Table 1.

[1] Research done in part at the Multiple Mirror Telescope, operated jointly by the Smithsonian Astrophysical Observatory and the University of Arizona.

TABLE 1

NON-SEYFERT, NONINTERACTING GALAXIES WITH $L > 10^{10}\ L_{\odot}$ AND 60/100 MICRON FLUX RATIO >0.5

NGC	Type	R.A.	Decl.	*B*-Magnitude	Date	Telescope[a] (m)
253.....	Sc(s)	$00^h45^m08^s$	−25°33′.7	8.13	1987 Oct 8	1.5
922.....	Sc(s)II.2pec	02 22 49	−25 01.1	12.55	1987 Oct 6	2.3
2146.....	SbIIpec	06 10 45	+78 22.5	11.24	1988 Jan 7	2.3
2764.....	Amor or Sbpec	09 05 27	+21 38.7	13.40	1988 Apr 1	1.5
2782.....	Sa(s)pec	09 10 54	+40 19.3	12.15	1988 Apr 2	1.5
2990.....	ScII:	09 43 40	+05 56.6	13.20	1988 Apr 5	1.5
3310.....	Sbc(r)pec	10 35 39	+53 45.9	11.20	1988 Apr 2	1.5
3504.....	Sb(s)/SBb(s)I–II	11 00 29	+28 14.5	11.80	1988 Apr 1	1.5
4433.....	SbcIII	12 25 03	−08 00.3	13.01	1988 Apr 2	1.5
4536.....	Sc(s)I	12 31 54	+02 27.7	11.01	1988 May 27	1.5
5653.....	Sc(s)IIIpec	14 28 01	+31 26.3	12.90	1988 Apr 1	1.5
5665.....	Sc(s)IVpec	14 29 58	+08 18.0	12.79	1988 Apr 1	1.5
5713.....	Sbc(s)pec	14 37 38	−00 04.5	12.00	1988 Apr 2	1.5
5861.....	Sc(s)II	15 06 33	−11 07.9	12.31	Not observed	...
5936.....	Sc(r)I–II	15 27 39	−13 09.6	13.00	1988 Jun 4	1.5
6574.....	Sbc(s)II.3	18 09 35	+14 58.2	12.85	1988 Apr 2	1.5

[a] Steward Observatory.

Observations were made at the Steward Observatory 61 inch (1.5 m) and 90 inch (2.3 m) telescopes on Mount Bigelow and Kitt Peak, respectively, using a 64 × 64 Rockwell hybrid focal-plane HgCdTe array (Rieke, Rieke, and Montgomery 1987). Pixel sizes were 1″.2 on the former telescope and 0″.85 on the latter. Fifteen of the 16 galaxies were observed over an 8 month period; only NGC 5861 could not be observed because of weather and time constraints (see Table 1).

III. DATA REDUCTION

A number of steps went into the data reduction. For flat-fielding to a few parts in 10^4, sky frames were taken interspersed with the data frames. The data frames were then ratioed against the adjacent sky frame as described by Rieke, Rieke, and Montgomery (1987). Pixels that responded far from the norm for the array were identified as "bad" and were removed, with their measured values replaced by the average from the surrounding pixels. In this process, approximately 50 of the highest and 50 of the lowest pixels are removed from each frame. The array used in the infrared camera has a dark current of less than 50 electrons per second, far below the photocurrent from the sky; hence, no corrections were required for the dark current.

The well depth of the array is large, about 5×10^6 electrons, making possible integration times of 30–80 s. As a result, the individual frames detected the galactic nuclei at high signal-to-noise ratio, and the nuclear image could be used to measure accurately the position of the galaxy on each frame. The galaxy frames were shifted to the average centroided position of all frames for that wavelength and co-added to yield the final *H* and *K* frames for each galaxy.

The presence of an obvious bar can sometimes be determined by looking at a contour plot of galaxy surface brightness ellipses and searching for features with an aspect ratio of 2.5:1 or better. However, a more sophisticated and potentially less biased search for subtle features is to use a set of programs known as the "Galaxy Surface Photometry" (GASP) package (Cawson 1983). The portion of GASP primarily used in this project determines galaxy surface brightness and ellipticity profiles useful in searching for a bar.

The input parameters used in GASP for each galaxy frame are the *x*-*y* center of the galaxy in the image, the galaxy semi-major axis and position angle, and the ellipticity of the image. Of these parameters, only the center position of the galaxy was explicitly input. The program itself chooses initial values for the orientation of the major axis and ellipticity. We avoided choosing input parameters for the major-axis orientation or the ellipticity, since gross values characteristic for the galaxy as a whole might be quite uncharacteristic for the inner region. The other input parameters common to all galaxies are given in Table 2.

The program samples the pixels around the ellipse given by the setup parameters. Pixel value variations are evaluated by the program as a function of the angle from the major axis. A Fourier transformation of this periodic function is performed to evaluate whether the ellipse parameters are correct. If the ellipse parameters are not correct, they are adjusted using the magnitudes of the Fourier components. In practice, only one ellipse parameter, the parameter corresponding to the largest coefficient, is adjusted per iteration. The process is repeated until the fit is sufficiently good to pass a residual test or when the ellipses reach the sky limiting surface brightness. The final outputs are surface brightness, an elliptical isophote map, ellipticity as a function of radius, position angle as a function of radius, and *x* and *y* position of the centers of the ellipses as a function of radius.

TABLE 2

INPUT PARAMETERS FOR GALAXY SURFACE PHOTOMETRY PACKAGE

Parameter	Value
Ratio between successive major axes	1.10
Minimum number of iterations	5
Maximum number of iterations	50
Threshold above sky to stop profile	0
Maximum factor by which profile can increase	1.5
Maximum fraction of ellipse inside frame	0.60
Maximum residual factor	0.0001
Maximum shift of center per iteration	0.50
Maximum shift of ellipticity per iteration	0.020
Maximum rotation of angle per iteration	1.0

IV. ANALYSIS OF GASP RESULTS

The output values of these parameters from GASP were used to search for characteristics of barred structures. In the central seeing disk region, the ellipticity should be small and the orientation of the axis should be fairly random and highly variable. The direction of the axis orientation as determined by GASP should probably not be correlated with the overall galaxy orientation. After a few iterations the seeing disk is exceeded and the GASP parameters should become more characteristic of the inner region.

The signature of a bar in the inner region should be a significant increase in ellipticity to a large value. Except in some specialized situations for galaxies at large inclinations, this rise in ellipticity should be correlated with a constant position angle at the same location. The ellipticity value corresponding to a bar should be higher than the ellipticity of the galaxy farther from the center, which corresponds to the overall ellipticity of the galaxy isophotes due to the galaxy's inclination.

The parameters of 15 galaxies were determined using GASP applied to the co-added H and K images seen in Figures 1–6. These parameters were adjusted to allow GASP to run 10–50 iterations per ellipse. The program parameters were set so that the program terminated for each galaxy through goodness-of-fit criteria rather than at the sky brightness level. Thus the outer few surface brightness contours may be spurious and uncharacteristic of the galaxy.

To test the way in which GASP will characterize the surface brightness of barred galaxies, two galaxies with known bars, NGC 1068 and NGC 2523, were imaged with the 2 μm camera (Fig. 1) and analyzed with GASP (Fig. 7). For the well-known Seyfert galaxy NGC 1068, with a small bar, the ellipticity drops sharply in the first four pixels, probably because of the intensity of the nucleus, then rises again to a value near 0.5. In the region where the ellipticity is rising, the position angle is constant, indicative of a bar. Farther out, the ellipticity decreases to a value more consistent with a low inclination system. NGC 2523 is a galaxy with a large, prominent bar and ring structure easily seen in optical photographs. The GASP analysis of NGC 2523 (Fig. 7) shows a large increase in ellipticity coupled with a constant position angle. This effect is present at both H and K bands. The bar is present out to about 25 pixels from the center. The drop in ellipticity at the last data point occurs outside the barred region. The combination of a trend of increasing ellipticity coupled with a constant position angle over this same region is a hallmark of a bar and is well illustrated by these two examples.

In general, the H and K GASP results were qualitatively consistent with each other for all of the GASP parameters: surface brightness shape, elliptical isophotes, ellipticity, position angle, and position of center. In a few cases, the final co-added H or K image was unsuitable for use with GASP, since the galaxy was too close to the sky background for GASP

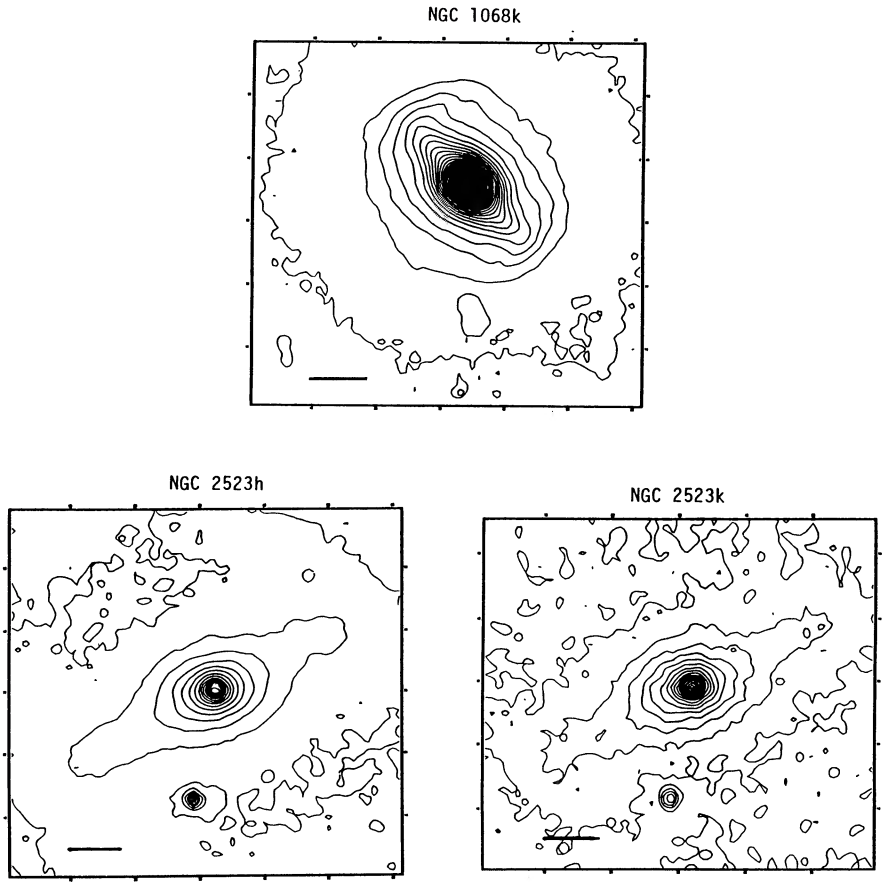

FIG. 1.—Contour maps of the galaxies NGC 1068 and NGC 2523. The h or k after the galaxy name signifies either the H (1.6 μm) or the K band (2.2 μm). The bar is 10′ in length.

to work successfully. The GASP profiles for the individual galaxies are illustrated in Figures 8–14 and are discussed below.

NGC 253 has an inclination of 73°, so any barred structure would be severely foreshortened. However, the galaxy is close enough (3 Mpc) that very high spatial resolution can be obtained, in partial compensation for the effects of the inclination. Because of the large size of the galaxy, our analysis was based on a 128 × 128 mosaic of 64 × 64 frames. In this galaxy the ellipticity is high at the center, as would be expected because the seeing disk and bulge are dominated by the highly inclined disk. The ellipticity rises a few pixels away from the center and remains elevated for a length of only a few pixels. The position angle in this region is nearly identical to the overall position angle of the galaxy. The position angle varies with increasing radius, not in accordance with the expected behavior for a bar. Visual inspection of the image does not reveal any linear structure aligned with the nucleus. In summary, we find no evidence for a bar. This conclusion is not in agreement with Scoville *et al.* (1985), who obtained a map at

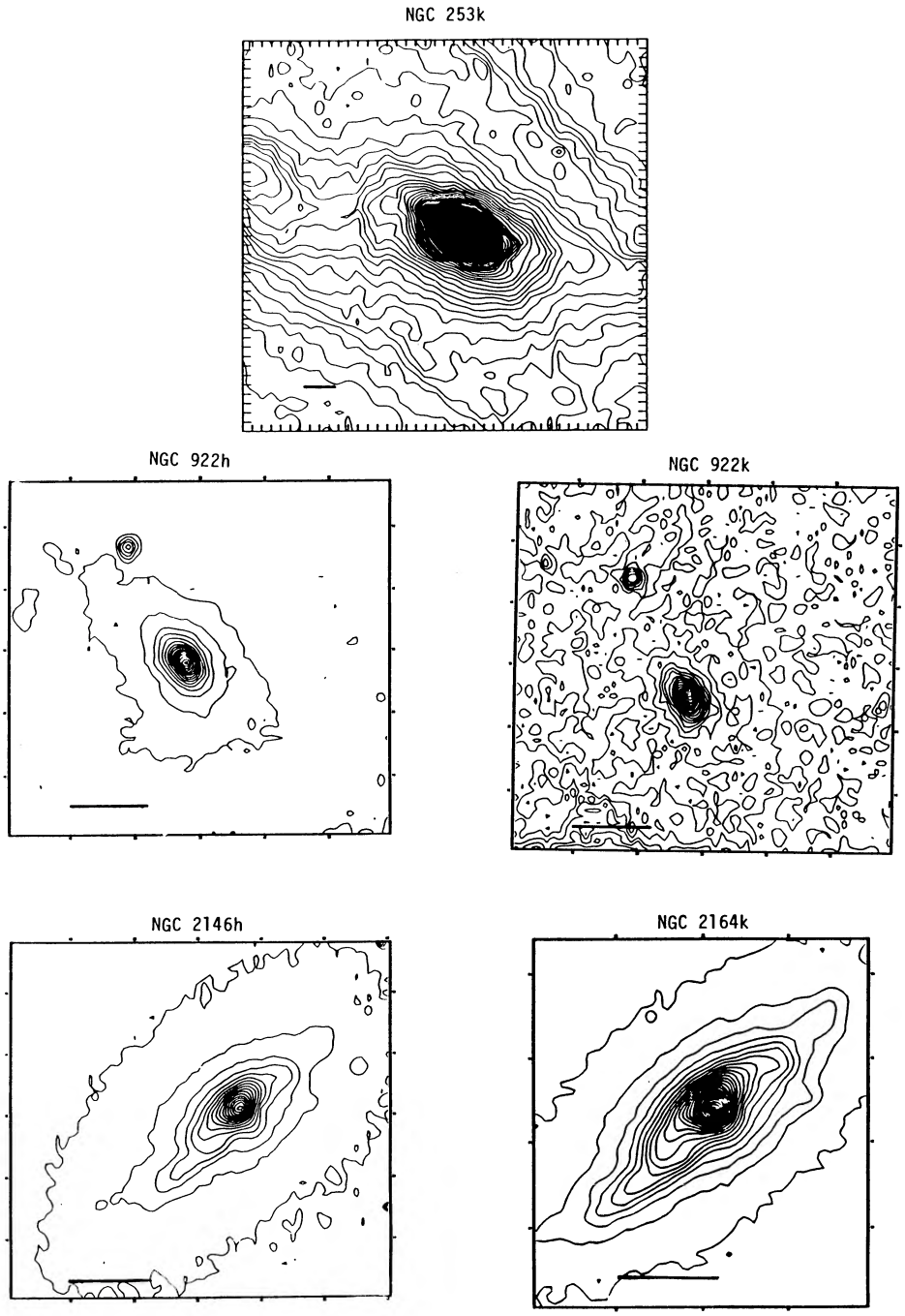

FIG. 2.—Contour maps of the galaxies NGC 253, NGC 922, and NGC 2146. The h or k after the galaxy name signifies either the H (1.6 μm) or the K band (2.2 μm). The bar is 10′ in length.

10″ resolution which appears to show a bar. The higher resolution of our map clearly shows the feature identified by them to bend sharply as it enters the nuclear region and not to be aligned with the nucleus. It therefore appears to be a spiral arm not a bar.

The GASP output for NGC 922 shows only a moderate rise in ellipticity from the center outward, indicative of the inclination of the galaxy. The lower ellipticity in the center is probably due to the contribution of the bulge to the surface brightness. The position angle is constant throughout, with a value of about 60°. Thus, there is no indication of a bar.

For NGC 2146 the H and K images show good overall agreement among the GASP derived parameters. The ellipticity rises to a maximum at about 10 pixels from the center. The position angle is constant at an angle of $-45°$, except for the centermost pixels.These changes are similar to what would be expected for a bar. However, if there were a bar, it would have a larger ellipticity than the galaxy would have for its final outer isophote. Since the ellipticity for this galaxy gradually rises to the value consistent with its inclination, the presence of a bar is unlikely.

For NGC 2764 there is good agreement between the ellip-

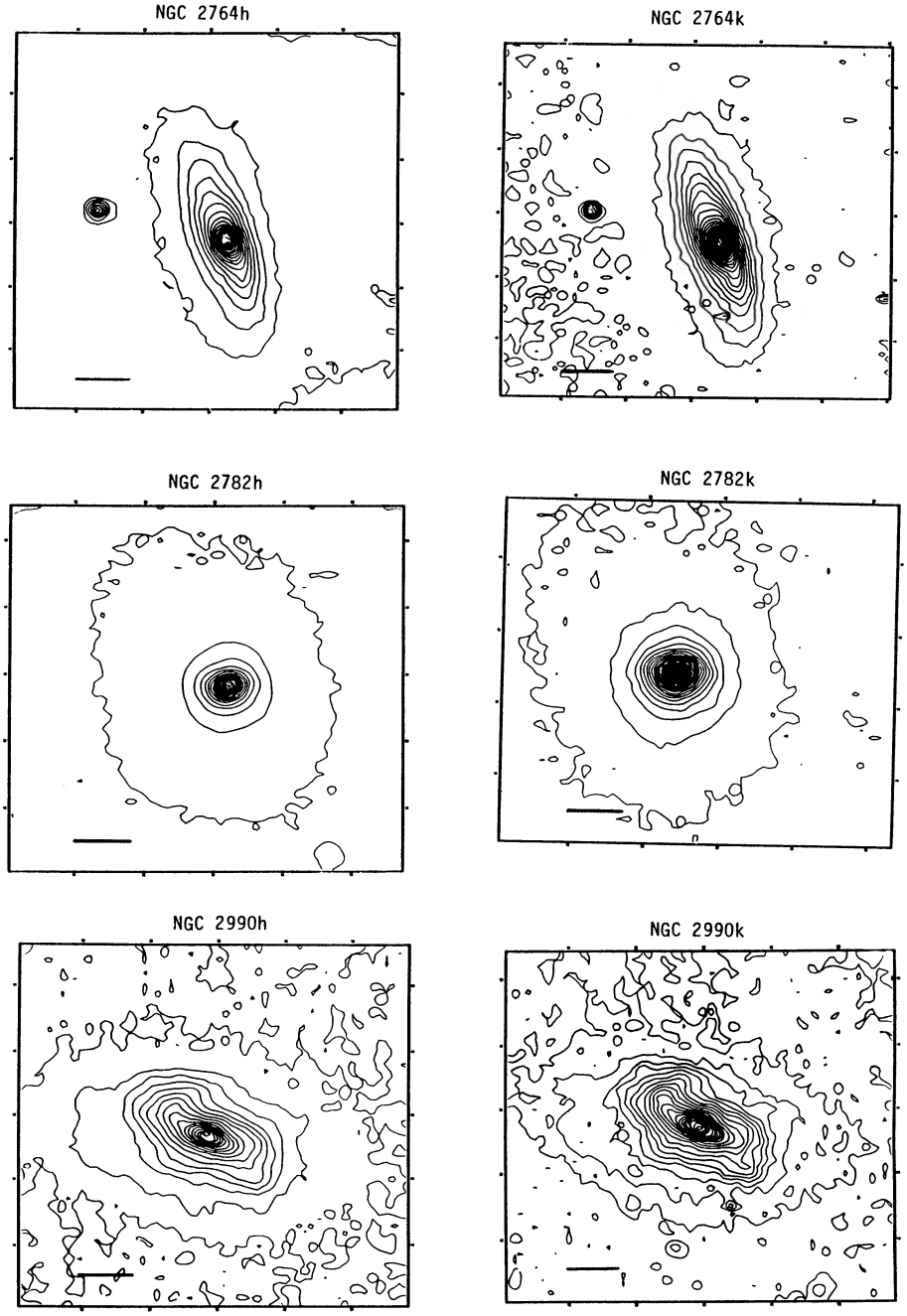

FIG. 3.—Contour maps of the galaxies NGC 2674, NGC 2782, and NGC 2990. The h or k after the galaxy name signifies either the H (1.6 μm) or the K band (2.2 μm). The bar is 10′ in length.

ticity plots and the position-angle plots between the H and K frames. The ellipticity rises slowly from the center to a maximum value of 0.7 about 15 pixels from the center. The position angle remains relatively constant except for the center few pixels. Thus, the change in ellipticity is due to the inclination of the galaxy. In the center area the bright bulge dominates and lowers the ellipticity. This case is somewhat ambiguous because of the high inclination of the galaxy.

In the case of NGC 2782, there is a strong correspondence between the H and K-band results. However, the values of the position angles change rapidly with radius, for both bands. Where the ellipticity first rises (reaching a maximum about 3 pixels from the center at H and K), the position angle is relatively constant, averaging a value of $-10°$. This could be representative of a possible bar structure, except that the ellipticity is too low, reaching a maximum of only 0.2, and the inner few pixels may only reflect seeing effects. A second maximum in the ellipticity is seen at about 25 pixels from the center at both H and K. These positions correspond to a region of constant position angles. However, the ellipticity is still too low for a bar to be present. The ellipticity remains constant for only a few pixels before the edge of the frame is reached.

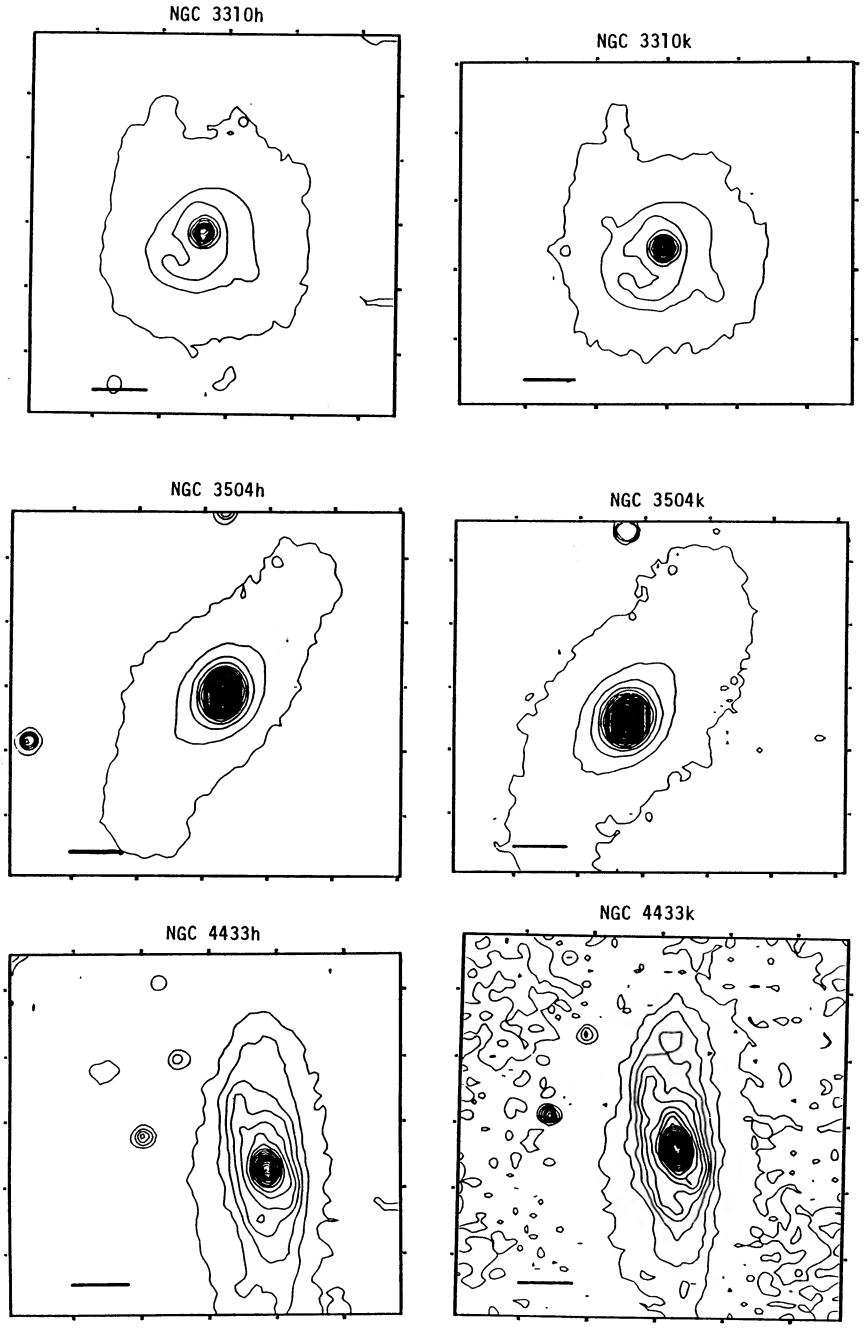

FIG. 4.—Contour maps of the galaxies NGC 3310, NGC 3504, and NGC 4433. The h or k after the galaxy name signifies either the H (1.6 μm) or the K band (2.2 μm). The bar is 10′ in length.

The images of NGC 2990 at H and K show striking similarities between the two bands. In both bands, the ellipticity begins at the center at a relatively large value of 0.4 and continues to increase to a maximum of 0.6 about 5 pixels from the center. The position angles of the isophotes in this central region are fairly constant. The isophotal plot shows an inner elongated region at a different position angle than the outer isophotes; the inclination is consistent with this rotation of position angle arising from geometric effects in a foreshortened barred galaxy. Thus, the basic prerequisites for a bar seem to be met. However, both the H and K frames appear to show two spiral arms coming out from the center. Inner spiral arms thus mimic many of the parameters present in a bar.

In NGC 3310 there is a sharp rise in the ellipticity to a maximum of nearly 0.5 at a distance of 5 pixels from the center. At 5 pixels the position angle of the ellipses shifts significantly. In both the H and K contour maps, the inner spiral arms can be seen. In contrast to NGC 2990, the coordinates of the center position of the ellipses also begin changing at the same position 5 pixels from the center. A change in the center coordi-

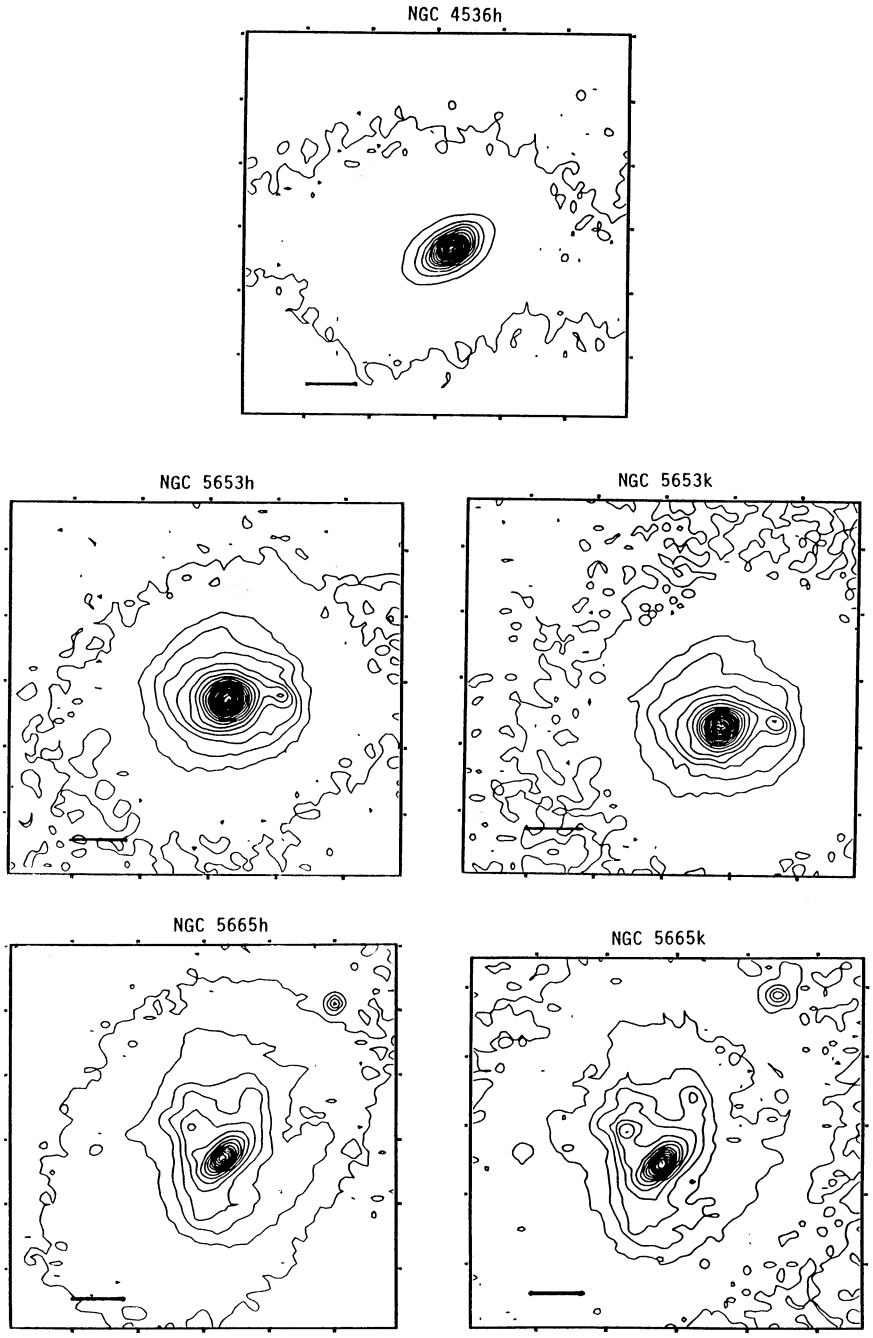

FIG. 5.—Contour maps of the galaxies NGC 4536, NGC 5653, and NGC 5665. The h or k after the galaxy name signifies either the H (1.6 μm) or the K band (2.2 μm). The bar is 10′ in length,

nates of the isophotal ellipses is a further indication of spiral arms. No evidence for a bar interior to the inner spiral arms is seen.

NGC 3504 shows good agreement between the *H* and *K* GASP results. The ellipticity shows a gradual increase to large values after the first 5 pixels. Similarly, the position angle is gradually increasing and then levels off. This behavior could indicate either a bar or a highly inclined galaxy; however, comparison of the ellipticity toward the edge of our frame with the ellipticity of the galaxy as a whole in optical photographs shows that the galaxy is not highly inclined and it therefore has a bar that extends into the nucleus.

In the *H* frame analysis of NGC 4433, the position angle for the ellipses remains constant at a value of about +85° from the center to the edge of the galaxy. The ellipticity rises gradually from about 0.1 at the center to about 0.7. Because the ellipticity is small in the inner regions, there is no evidence for a bar. This is a highly inclined system, so the final ellipticity at the edge reflects the inclination of the galaxy.

NGC 4536 shows a possible bar, oval distortion, or inner

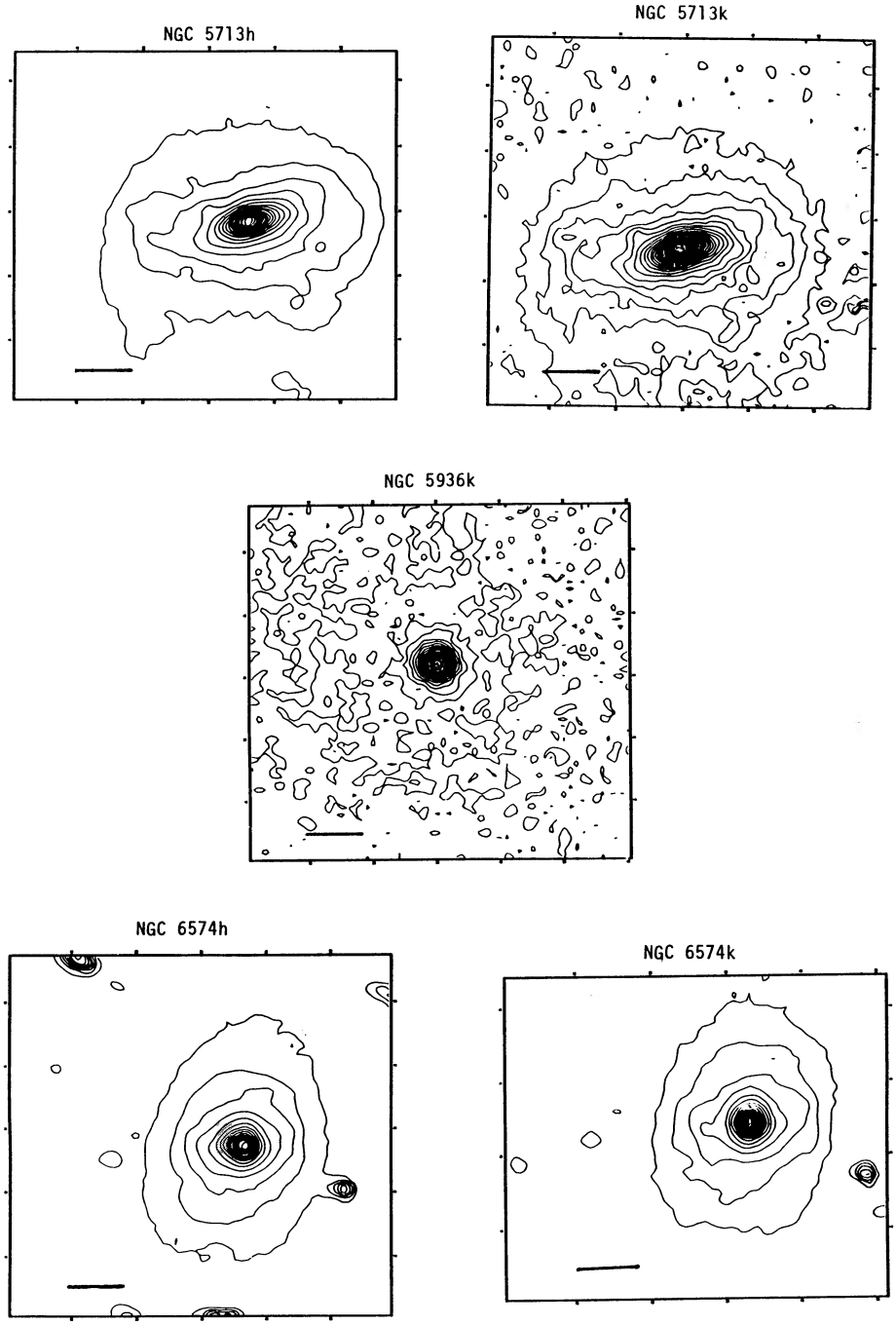

FIG. 6.—Contour maps of the galaxies NGC 5713, NGC 5936, and NGC 6574. The h or k after the galaxy name signifies either the *H* (1.6 μm) or the *K* band (2.2 μm). The bar is 10′ in length.

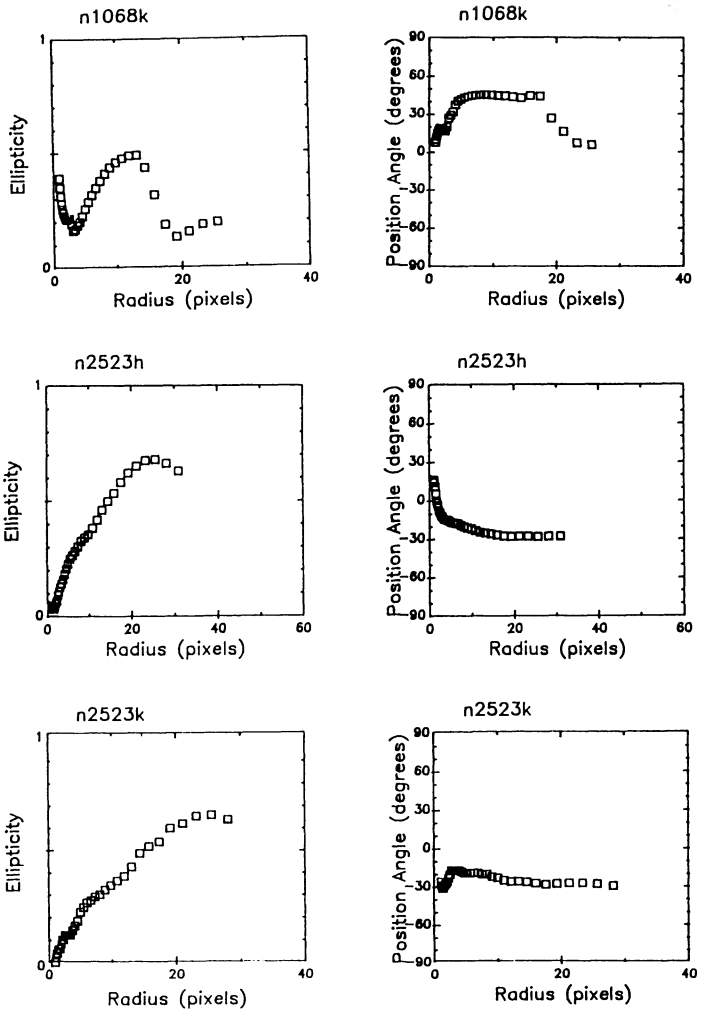

FIG. 7.—Plots of ellipticity and position angle generated by the GASP package for the galaxies NGC 1068 and NGC 2523.

spiral arms extending to about 10 pixels from the center. The ellipticity increases to about 0.4, while the position angle is constant in the region around 10 pixels. The position angle does change substantially from the center to about 6 pixels, but reaches a constant value in the region of high ellipticity. These characteristics are indicative of a bar.

NGC 5653 shows a rapid rise in ellipticity that is correlated with a changing position angle. This behavior is a trademark of spiral arms. The effect is present in both the *H* and *K* frames. Contour plots also show the inner spiral arms.

NGC 5665 shows a moderate increase in ellipticity in the first 5 pixels coupled with a reasonably constant position angle over this region. These trends are present at both *H* and *K*, and are indicative of a small bar. Outside this region the ellipticity decreases dramatically and then increases dramatically, indicative of more complex structure, sucn as spiral arms extending from the end of the bar. However, the possible bar seems to be aligned almost exactly along the major axis of the galaxy, casting some doubt on its existence.

NGC 5713 shows a moderate increase in ellipticity to about 0.5 in a region where the position angle is constant. The parameters derived from the *H* and *K* frames agree well. However, the position angle is constant throughout the galaxy, indicating that we are probably seeing an inclination effect rather than a bar. We will classify it, however, as a possible bar.

NGC 5936 shows a very low ellipticity of about 0.1 or less for the inner 15 pixels of the galaxy. The position angle is rising dramatically over this region. This combination is not similar to the signature of a bar.

In NGC 6574 the ellipticity rises in spurts but never becomes greater than 0.4, which it reaches at the galaxy edge. The posi-

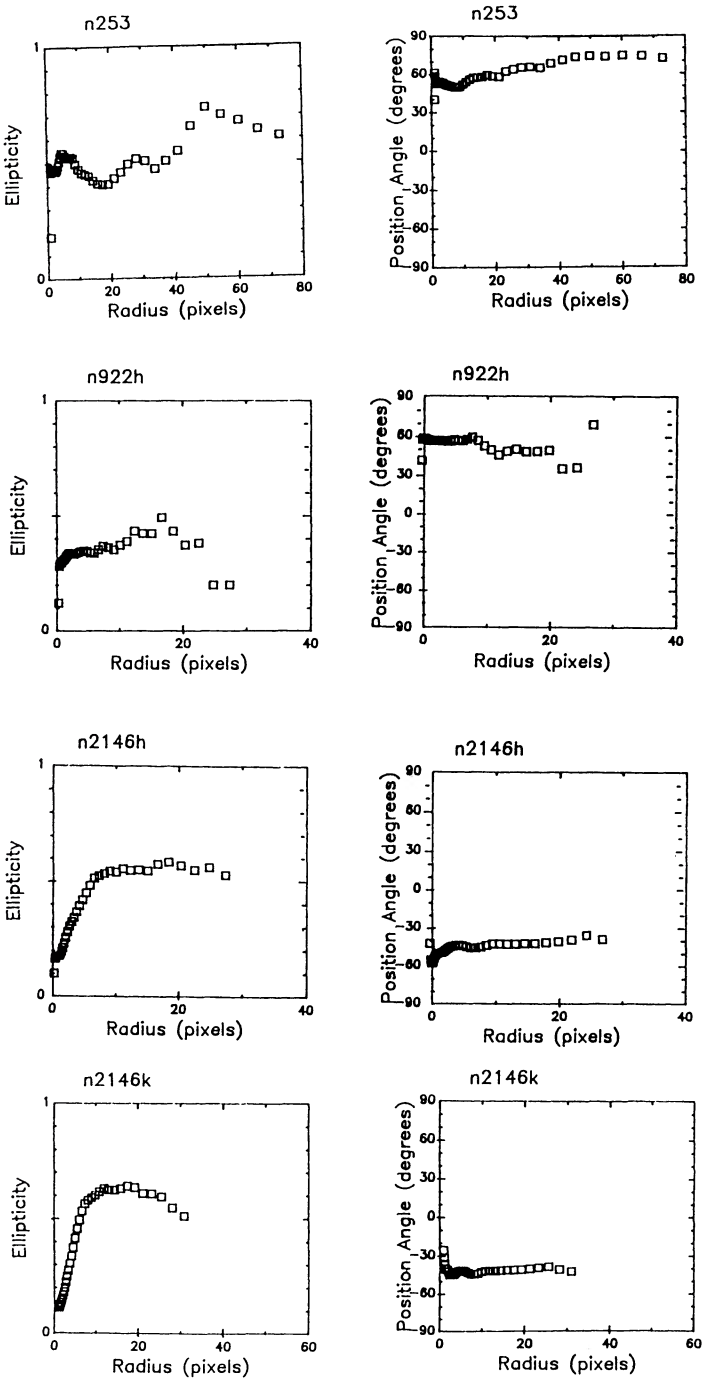

FIG. 8.—Plots of ellipticity and position angle generated by the GASP package for the galaxies NGC 253, NGC 922, and NGC 2146.

tion angle is constant only from about 4 to 8 pixels, a place where the ellipticity is increasing. The ellipticity is also low for a bar, reaching only 0.25 at H and 0.35 at K. We conclude that there is no bar present.

The classification by our techniques is given in Table 3 and is consistent in all cases with that listed in RSA. This result tends to verify our techniques and also indicates that few infrared-bright galaxies have bars hidden in the optical by young stars or obscuration. It should be noted that the morphologies of NGC 5653 and NGC 5665 are peculiar and may indicate margers and/or interactions of some degree.

V. MID-INFRARED OBSERVATIONS

The mid-infrared emission of these galaxies can be examined in further detail to ascertain whether it is centrally concentrated at 10 μm. If outlying disk emission is important, the role of the bar in stimulating emission would be less important, and alternative methods of stimulating starbursts in a galaxy's outer regions would be necessary. A comparison of ground-based, small-aperture photometry with the *IRAS* band 1 flux can help determine the degree of central concentration of the star formation activity. It would be ideal to compare ground-

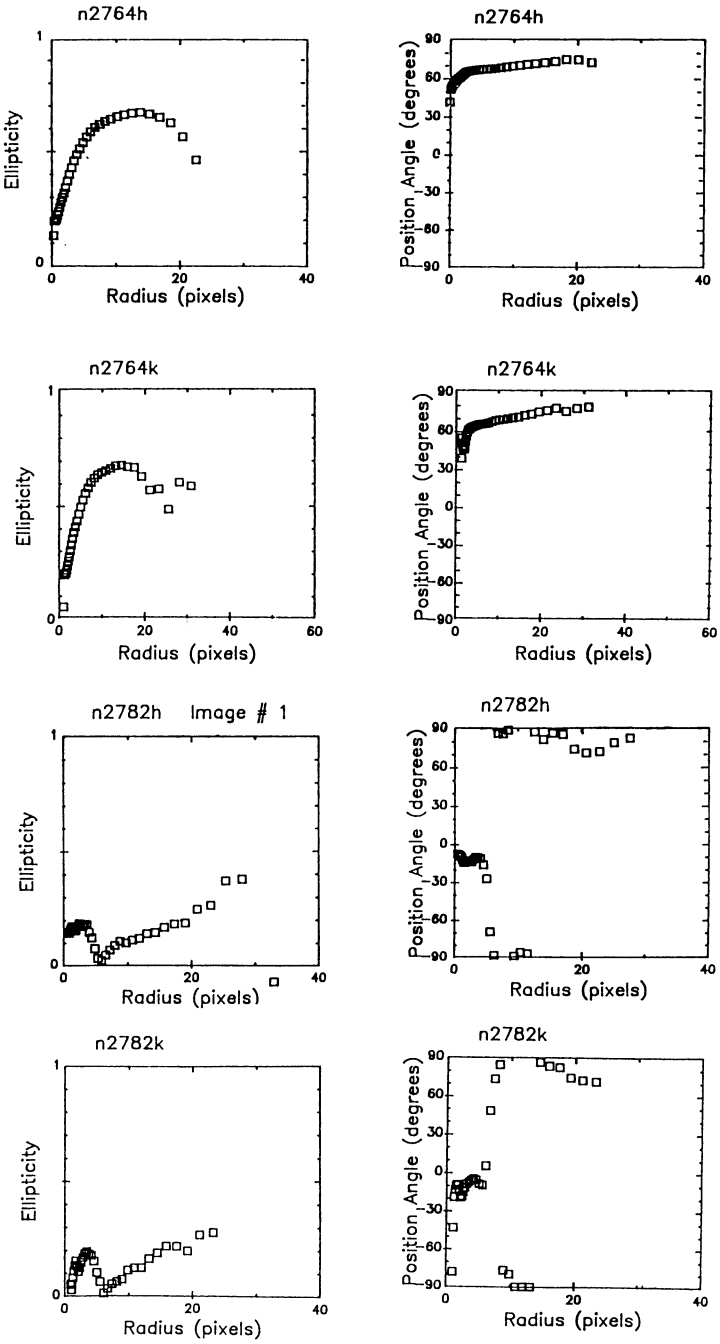

FIG. 9.—Plots of ellipticity and position angle generated by the GASP package for the galaxies NGC 2764 and NGC 2782.

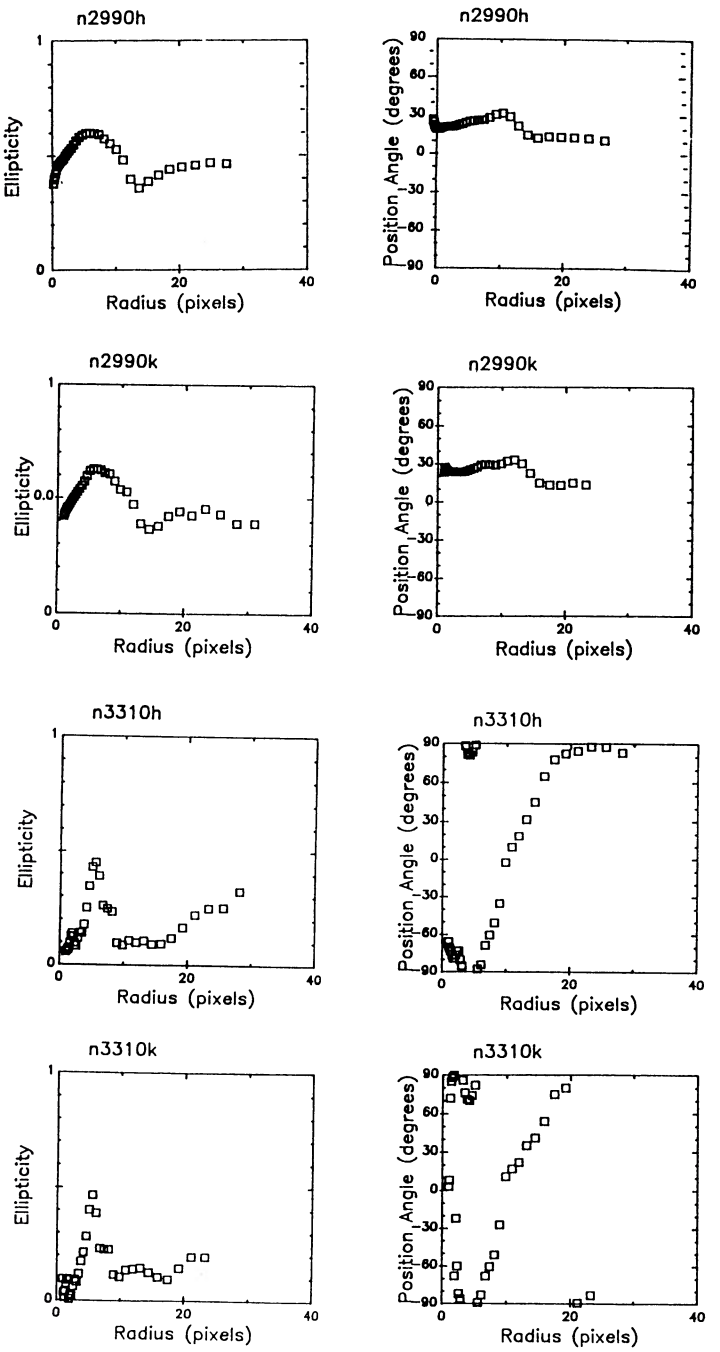

FIG. 10.—Plots of ellipticity and position angle generated by the GASP package for the galaxies NGC 2990 and NGC 3310.

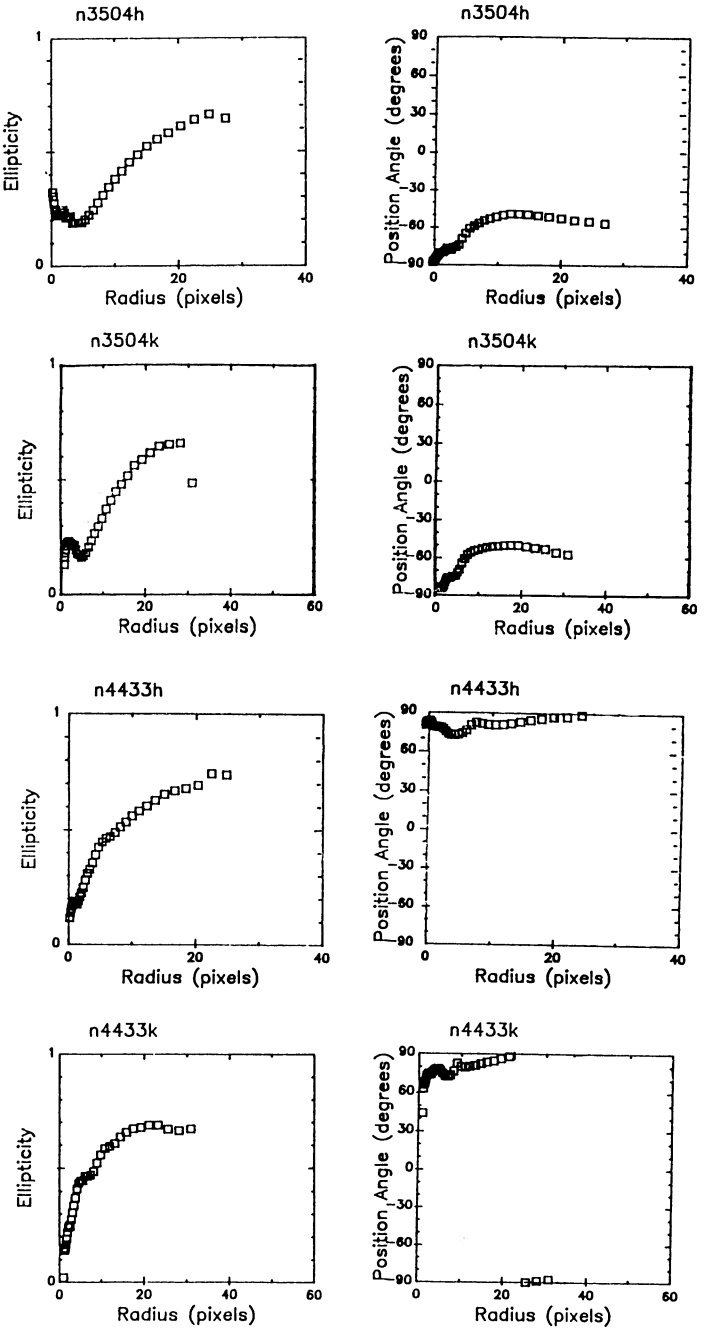

FIG. 11.—Plots of ellipticity and position angle generated by the GASP package for the galaxies NGC 3504 and NGC 4433.

based narrow band photometry near 12 μm, made with a small aperture, to the *IRAS* band 1 flux, which represents a much larger field of view but is at a similar effective wavelength. In this way, the ground-based measurement avoids the effects of polycyclic aromatic hydrocarbon emission features and/or silicate absorption. These features would be expected to have a strong effect on conventional *N*-band photomery at 10 μm and would tend to depress the flux compared with the *IRAS* measures, indicating less central concentration than actually exists.

We obtained narrow-band photometry with a small aperture (5″) of five of these galaxies, using a developmental bolometer system at the Multiple Mirror Telescope. The results of these observations are described in Table 4. For NGC 922, NGC 2782, and NGC 5936 the 12.5 μm narrow-band measurements are a substantial fraction of the *IRAS* band 1 measurement, indicating that the infrared emission at this wavelength is concentrated. The measurements for NGC 3310 and NGC 6574 show a less concentrated form of infrared emission. NGC 253 (Rieke and Low 1975), NGC 3504, and NGC 4536 (Rieke 1976; Telesco *et al.* 1987) can be shown from previous measurements to be centrally concentrated, whereas NGC 5665 and NGC 5861 (Devereux 1987*a*) are more extended. NGC 922 has also been measured by Devereux (1987*a*), but given the poor signal-to-noise ratio and his use of a broad-band *N*-band filter, the interpretation of this measurement is ambiguous.

Given that most normal *IRAS* galaxies are poorly concentrated, these measurements show that our initial selection criteria, which were based solely on high infrared luminosity and hot far-infrared colors, also tended to yield galaxies with nuclear emission (i.e., six of 10 cases are reasonably concentrated).

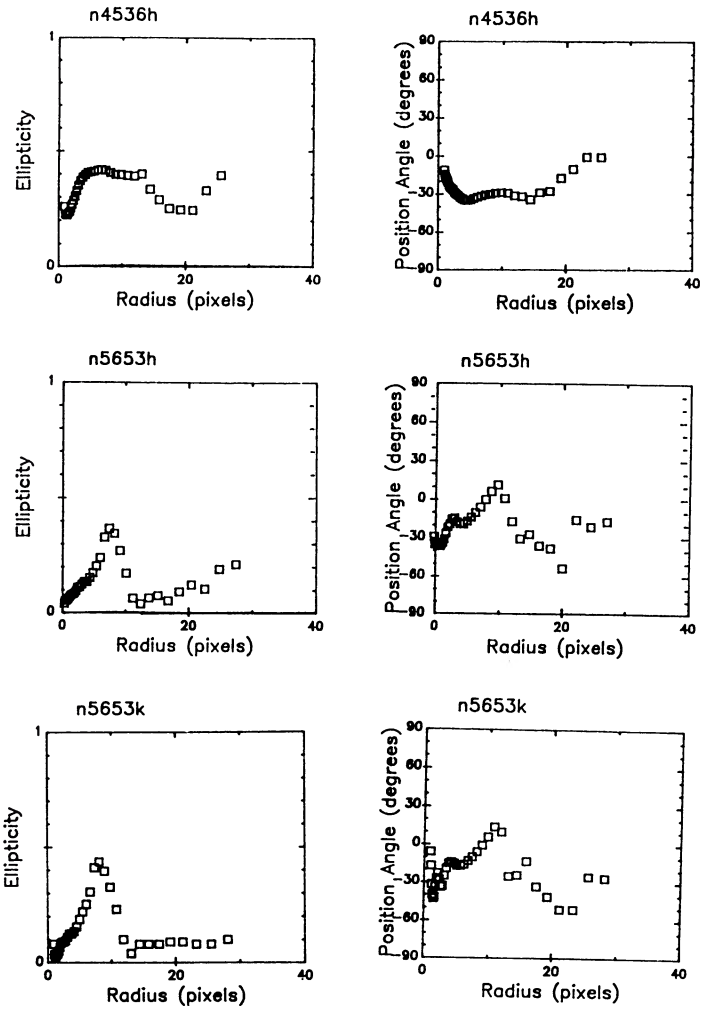

FIG. 12.—Plots of ellipticity and position angle generated by the GASP package for the galaxies NGC 4536 and NGC 5653.

VI. BARS AND INFRARED ACTIVITY

Of the 15 galaxies we have imaged, 10 pass the test for 25 μm excess proposed by Hawarden *et al.* (1986). However, only three of these galaxies are barred or possibly barred (NGC 3504, NGC 4536, and NGC 5713). Particularly good examples of unbarred galaxies with 25 μm excesses are NGC 253 and NGC 5936. Other cases include NGC 2146, NGC 2764, NGC 2782, NGC 3310, and NGC 4433. Some of the latter galaxies show evidence for weak interactions (e.g., NGC 2782) or are relatively difficult to classify because of high inclination (e.g., NGC 2146, NGC 2764, NGC 4433). Our study does not support the hypothesis of Hawarden *et al.* (1986) that bars are a ubiquitous feature of galaxies with 25 μm excesses. We find no evidence for a high prevalence of obscured or hidden bars that might accompany 25 μm excesses in optically unbarred galaxies.

Neither does it seem necessary that a bar be present to feed a nuclear starburst. Specific counterexamples from our sample are NGC 253, NGC 922, NGC 2782, and NGC 5936. Given the proportion of galaxies in the sample with concentrated nuclear emission, it is likely that additional examples will be found when the remaining five galaxies have adequate ground-based measures of nuclear concentration. If we assume that the nuclear concentration of infrared luminosity is the same as the concentration at 12 μm, NGC 2782 and NGC 5936 each produces $\sim 2 \times 10^{10}\ L_{\odot}$ within a central region of diameter ~ 1 kpc. NGC 253 produces a similar luminosity in a diameter of only ~ 300 pc. The density of energy production in these galaxies is therefore of the same order as in the prototypical starburst in M82.

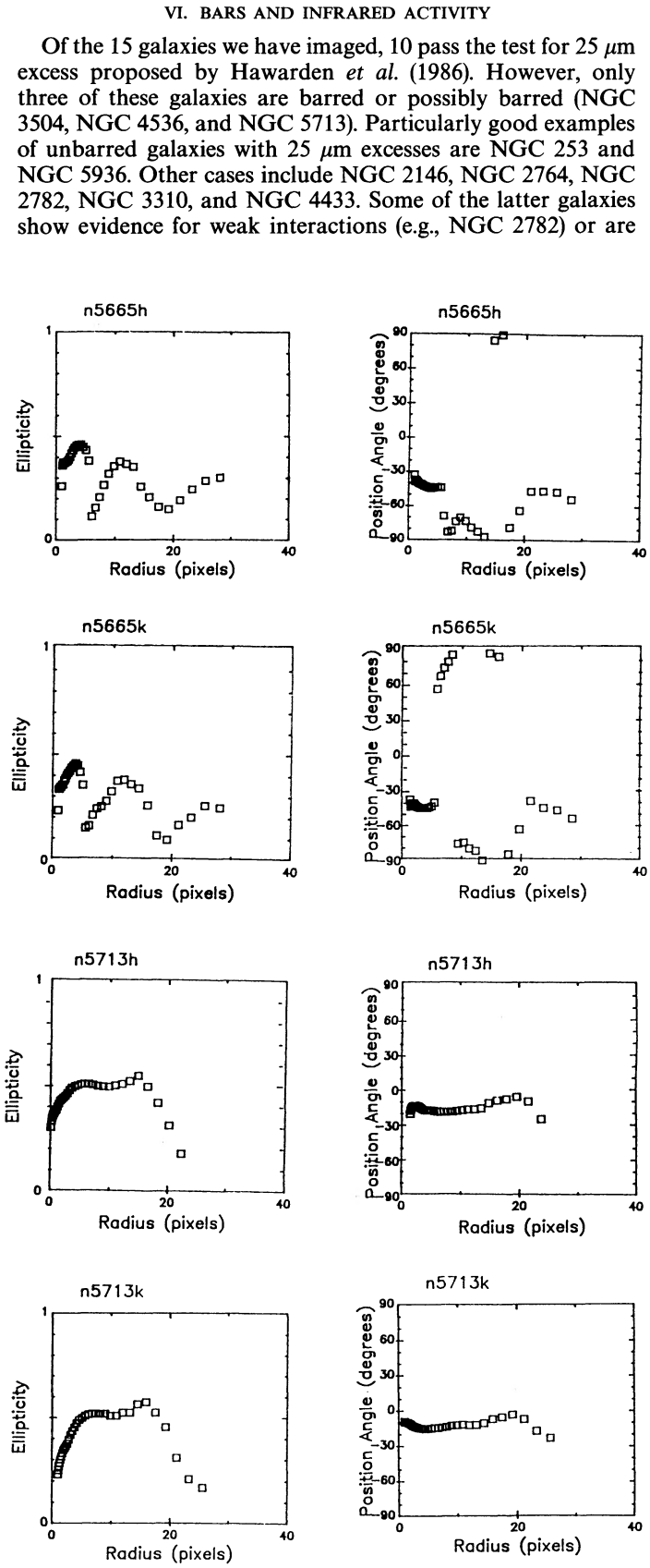

FIG. 13.—Plots of ellipticity and position angle generated by the GASP package for the galaxies NGC 5665 and NGC 5713.

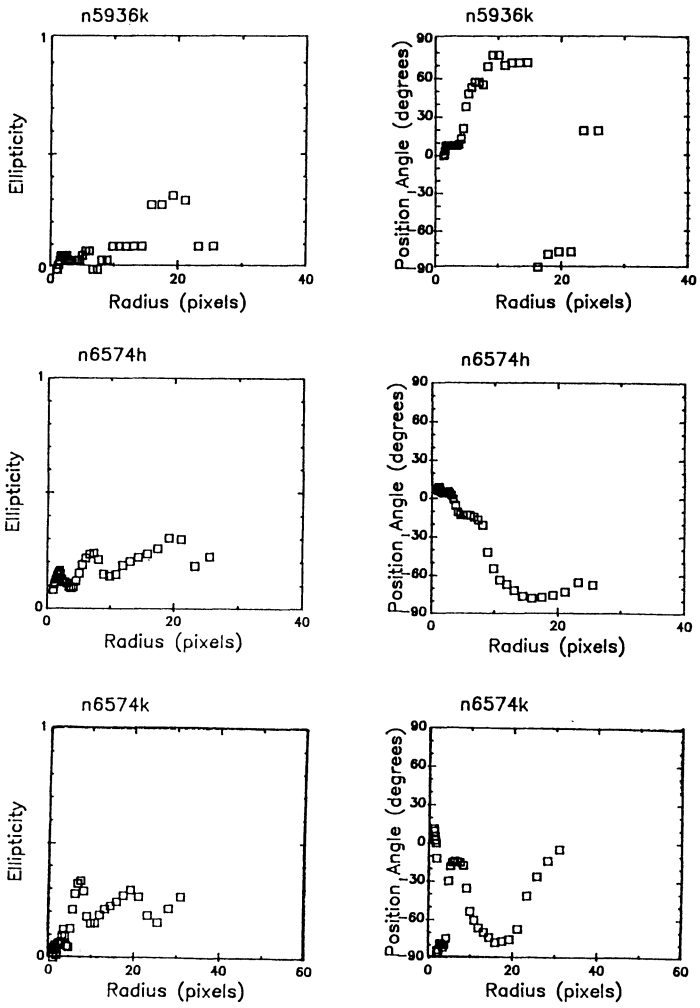

FIG. 14.—Plots of ellipticity and position angle generated by the GASP package for the galaxies NGC 5936 and NGC 6574.

TABLE 3

PROPERTIES OF GALAXIES

Galaxy (1)	D[a] (2)	Ellipticity[b] (3)	Inclination[c] (4)	Features[d] (5)
NGC 253.....	0.53	0.705	73	No bar, ISA
NGC 922.....	0.04	0.088	24	No bar
NGC 2146.....	0.20	0.369	51	No bar
NGC 2764.....	0.23	0.411	54	No bar, inclination
NGC 2782.....	0.12	0.241	41	No bar
NGC 2990.....	0.24	0.425	55	No bar, ISA
NGC 3310.....	0.09	0.187	36	No bar, ISA
NGC 3504.....	0.09	0.187	36	Bar
NGC 4433.....	0.32	0.521	61	No bar, inclination
NGC 4536.....	0.33	0.532	62	Possible bar, inclination, ISA
NGC 5653.....	0.07	0.149	32	No bar, ISA
NGC 5665.....	0.15	0.292	45	Possible bar
NGC 5713.....	0.05	0.109	27	Possible bar
NGC 5861.....	0.23	0.411	54	Not observed
NGC 5936.....	0.03	0.067	21	No bar
NGC 6574.....	0.10	0.206	37	No bar

[a] D = log (major/minor) axis radii in arcminutes. From de Vaucouleurs, de Vaucouleurs, and Corwin 1976.

[b] Ellipticity = $1 - (b/a)$, where b is the semiminor axis and a is the semimajor axis.

[c] Inclination (0 = face-on) determined from the ellipticity values in col. (3).

[d] Features determined to be present from analysis of GASP parameter. "Inclination" means that inclination makes determination of a bar difficult. ISA = inner spiral arms.

TABLE 4

10 MICRON WINDOW MEASUREMENTS

Galaxy	IRAS Band 1 (Jy)	N (Jy)	12.5 μm (Jy)	13.3 μm (Jy)	12.5 μm/Band 1 (%)
NGC 922.....	0.29	...	0.126 ± 0.38	...	43
NGC 2782.....	0.51	0.08 ± 0.007	0.40 ± 0.043	0.29 ± 0.086	78
NGC 3310.....	1.25	0.05 ± 0.008	0.17 ± 0.042	...	14
NGC 5936.....	0.48	...	0.15 ± 0.030	0.20 ± 0.032	31
NGC 6574.....	0.93	...	0.06 ± 0.017	...	6

VII. CONCLUSION

We have used deep near-infrared images and the GASP program to search for barred structure in infrared-luminous, star-forming galaxies. Of 15 optically unbarred or possibly barred infrared-luminous galaxies, four galaxies (NGC 3504, NGC 4536, NGC 5665, and NGC 5713) showed features in ellipticity and position angle indicative of bars. Spiral arms coming out of the nucleus, but no bars, were seen in NGC 253, NGC 2990, NGC 3310, and NGC 5663. These arms mimic the ellipticity profile for bars, but show a variable position angle. From an initial sample of 22 infrared-selected galaxies, at last eight do not have strong bars (results for two more are inconclusive because of the effect of high inclination). This result is consistent with the presence of a higher proportion of barred galaxies in infrared-selected samples than the 35% that is typical of spirals in general. However, within our sample, there are unbarred and noninteracting galaxies that have 25 μm excesses above the threshold where Hawarden *et al.* (1986) have argued that bars are ubiquitous. In addition, there are similar galaxies with central starbursts producing infrared luminosities of $2 \times 10^{10}\ L_{\odot}$ or greater emerging from regions of 1 kpc or less in diameter in their nuclei. These results show that bars are not a necessary prerequisite for strong infrared activity in isolated galaxies.

This work was supported in part by the NASA SADAP/IRAS Data Analysis Program and in part by the National Science Foundation. We thank M. Rieke for assistance in obtaining the infrared camera frames and E. Montgomery, M. Rieke, and Rockwell International Science Center for their work in constructing the camera. We also thank D. Zaritsky for constructive comments on an earlier version of this manuscript.

REFERENCES

Arsenault, R. 1989, *Astr. Ap.*, **217**, 66.
Cawson, M. G. M. 1983, Ph.D. thesis, University of Cambridge.
de Vaucouleurs, G., de Vaucouleurs, A., and Corwin, H. G. 1976, *Second Reference Catalog of Bright Galaxies* (Austin: University of Texas Press).
Devereux, N. 1987*a*, *Ap. J.*, **323**, 91.
Devereux, N. 1987*b*, in *Star Formation in Galaxies*, ed. C. J. L. Persson (NASA CP-2466), p. 219.
Hawarden, T. G., Mountain, C. M., Leggett, S. K., and Puxley, P. J. 1986, *M.N.R.A.S.*, **222**, 41.
Hummel, E., van der Hulst, J. M., and Dickey, J. M. 1984, *Astr. Ap.*, **134**, 207.

Norman, C. A. 1987, in *Star Formation in Galaxies*, ed. C. J. L. Persson (NASA CP-2466), p. 395.
Puxley, P. J., Hawarden, T. G., Mountain, C. M., and Leggett, S. K. 1987, in *Star Formation in Galaxies*, ed. C. J. L. Persson (NASA CP-2466), p. 619.
Rieke, G. H. 1976, *Ap. J. (Letters)*, **206**, L15.
Rieke, G. H., and Lebofsky, M. J. 1986, *Ap. J.*, **304**, 326.
Rieke, G. H., and Low, F. J. 1975, *Ap. J.*, **197**, 17.
Rieke, M. J., Rieke, G. H., and Montgomery, E. F. 1987, in *Infrared Astronomy with Arrays*, ed. C. G. Wynn-Williams and E. E. Becklin (Honolulu: University of Hawaii), p. 213.
Roberts, W. W., Huntley, J. M., and van Albada, G. D. 1979, *Ap. J.*, **233**, 67.
Sandage, A., and Tammann, G. A. 1981, *A Revised Shapley-Ames Catalog of Bright Galaxies* (Carnegie Inst. Washington Pub. 635) (RS).
Scoville, N. Z., Soifer, B. T., Neugebauer, G., Young, J. S., Matthews, K., and Yerka, J. 1985, *Ap. J.*, **289**, 129.
Sellwood, J. A. 1981, *Astr. Ap.*, **99**, 362.
Telesco, C. M., Decher, R. Ramsey, B. D., Wolstencroft, R. D., and Leggett, S. G. 1987, in *Star Formation in Galaxies*, ed. C. J. L. Persson (NASA CP-2466), p. 497.
Telesco, C. M., and Gatley, I. 1984, *Ap. J.*, **284**, 557.
Véron-Cetty, M.-P., and Véron, P. 1987, *A Catalogue of Quasars and Active Nuclei* (3d ed.; ESO Scientific Report).
Zaritsky, D., and Lo, K. Y. 1986, *Ap. J.*, **303**, 66.

STEPHEN M. POMPEA and G. H. RIEKE: Steward Observatory, University of Arizona, Tucson, AZ 85721